Title

Benefit of iodine density images to reduce out-of-field image artifacts at rapid kVp switching dual-energy CT.

Permalink

Journal

ISSN

Authors

Dotson, Brandan
Lambert, Jack W
Wang, Zhen J
et al.

Publication Date

DOI

Peer reviewed

Benefit of Iodine Density Images to Reduce Out-of-Field Image Artifacts at Rapid kVp Switching Dual Energy CT

Brandan Dotson, **Jack W. Lambert, PhD**, **Zhen J. Wang, MD**, **Yuxin Sun, MS**, **Michael A. Ohliger, MD, PhD**, **Sebastian Winklhofer, MD**, and **Benjamin M. Yeh, MD.**
Department of Radiology, University of California San Francisco, 505 Parnassus Avenue, San Francisco, CA 94143-0628

Abstract

Purpose—To evaluate the reduction of out-of-field artifacts caused by body parts outside the field of view (FOV) at rapid kVp switching dual energy CT (rsDECT).

Materials and methods—This retrospective study was approved by our institutional review board. Informed consent was not required. We viewed 246 consecutive rsDECT thoracoabdominal scans to identify those with body parts outside the maximal FOV of 50 cm. The maximal length, thickness and subjective severity of the out-of-field artifacts were recorded for the 40, 65 and 140 keV virtual monochromatic and the iodine and water density images. Artifact severity was rated on a 5 point scale from 0=absent to 5=obscures intraabdominal/intrathoracic anatomic detail. Artifact thickness and severity scores were compared by t-test and Wilcoxon tests, respectively.

Results—In 20 of 246 scans (8.1%), body parts extended past the maximum FOV of 50 cm. The mean BMI of these 20 patients was 40.2 kg/m^2 (range, 26.83 to 61.69 kg/m^2), and out-of-field artifacts occurred for all 20. The mean out-of-field artifact maximal length was 16.6 cm. The mean artifact thickness was significantly less for iodine density (0.6 mm) than for the 65 keV and water density images (8.4 and 13.5 mm, respectively, p<0.001 each comparison). The mean artifact severity score was lower for iodine density (0.2) than for the 65 keV and water density images (2.5 and 2.6, respectively, p<0.001 each).

Conclusion—Iodine density images reduce out-of-field image artifact at rsDECT and assists in the evaluation of peripheral tissues that extend beyond the maximal CT FOV.

Introduction

Computed tomography (CT) is a robust imaging modality that frequently shows less severe imaging artifact compared with what is seen with other cross-sectional imaging tests, including MRI and US. Nevertheless, image artifacts at CT can arise from many causes, including metal (1), motion (2), beam hardening (3), and out-of-field objects (4). Out-of-field objects result in excessive signal attribution to the voxels at the outer limits of the field of view (FOV) and limits evaluation of tissue in those regions. Out-of-field CT artifacts, also known as truncation artifacts, are increasingly common due to the increasing number of patients with large body habitus or who are unable to move their arms out of the imaged area (5). Several algorithms have been designed to mitigate this artifact, either via extrapolation of the projection data beyond the reconstructed FOV (6), extrapolation using morphological assumptions (7), extrapolation using adaptive detruncation (8), or via actual extension of the reconstructed FOV (9). Unfortunately to our knowledge none of these correction methods have been adopted for routine clinical use, and as such out-of-field artifacts remain prevalent.

Dual energy CT (DECT) involves the simultaneous acquisition of image data at two different x-ray energy spectra. These data are increasingly shown to provide diagnostic capabilities beyond that of conventional single energy CT (10). DECT can reduce artifacts resulting from beam hardening (11) and metal implants (12, 13). Material decomposition of DECT data can provide an iodine density image, which highlights contrast material signal, and a corresponding water density image, which simulates an unenhanced CT scan (14). The iodine density image is known to benefit many thoracoabdominal imaging indications, including to evaluate for possible pulmonary embolus (15), abdominal perfusion (16), and to detect hyper- or hypovascular masses in the liver and pancreas (17, 18). In addition to these diagnostic capabilities, iodine density images have also recently been shown to reduce intestinal peristalsis motion artifacts (19). Similar to motion artifact, out-of-field artifacts arise from errors in signal mapping at CT. Therefore, we hypothesized that out-of-field artifacts may be improved at DECT image reconstruction.

The aim of our study was to test whether DECT image reconstructions are also able to reduce out-of-field artifacts in scans where patient body parts extend beyond the maximum scan FOV.

Materials and methods

Our study was approved by our institutional review board and compliant with HIPAA policy.

Patients

We retrospectively identified 246 consecutive thoracoabdominopelvic DECT studies in unique patients obtained in our institution from April 2014 to December 2014. Scans were conducted using a rapid-switching DECT (rsDECT) scanner (CT Discovery 750HD, GE Healthcare, Waukesha, WI), operating with tube potentials of 80 and 140 kVp, helical acquisition mode with a pitch of 1.375:1 and a collimation of 40 mm (64 x 0.625 mm detector rows). The Gemstone Spectral Imaging (GSI) preset was selected to match the

CTDIvol of a single energy acquisition at 120 kVp with a Noise Index (GE's image quality reference parameter) of 31 defined at an image thickness of 1.25 mm. This is our clinical routine to ensure dose neutrality compared to single energy CT scans. Although some institutions set a size limit for patients for scanning with DECT, we have not set a patient size limit for DECT protocols in our hospital. These patients included 237 men and 9 women with a mean age of 65 years (range, 25 to 97). The skew toward men in our study reflects the patient population of our medical center, which services former military veterans. The indications for the CT scans were: abdominal pain (n=72), evaluation for possible malignancy (n=79), sepsis (n=18), and other (n=74). Patient height and weight were collected for the calculation of the body mass index (BMI). BMI was calculated as weight in kg divided by the square of the height in meters.

Imaging evaluation

All images were viewed on an Advantage Windows Workstation (AWS 4.5, GE Healthcare, Waukesha, WI). Each study was assessed for the presence of out-of-field artifacts that appeared as artifactually bright signal that was obviously brighter than that of adjacent similar tissue, most intense at the periphery of the FOV and crossed anatomic boundaries. The locations of artifact were classified as occurring on the left or right side, and in the chest, abdomen, pelvis, or limb. We measured the <u>chord length</u> of the artifact, which we defined to be the maximal straight line length of a contiguous artifact as seen on axial images (Fig 1a). The number of non-contiguous artifacts were recorded for each patient. The z-axis length of each artifact was recorded.

Further evaluation focused only the single artifact for each patient that showed the longest chord length on axial images. Two readers (BLIND and BLIND) by consensus viewed 40, 65, and 140 keV images as well as the iodine and water density images to record the following findings: <u>Artifact thickness</u> was recorded in centimeters (cm) as the maximal distance of the artifact measured perpendicularly inwards from the edge of the axial CT image (Fig 1b). <u>Artifact severity</u> was scored on the following scale: 0 = absent; 1 = visible artifact, does not obscure anatomy; 2 = obscures anatomy in subcutaneous fat, but not muscle; 3 = obscures anatomy of the subcutaneous fat and muscle, but not the intraperitoneal or intrathoracic anatomy; 4 = obscures less than 1 cm of anatomy deep to the pleura or peritoneum; and 5 = obscures more than 1 cm of anatomy in the thoracoabdominal cavity (Fig 2). Readers also recorded whether the out-of-field artifact obscured anatomy or disease in an area of clinical interest. We used consensus rather than independent readings since the parameters in our study do not assess diagnostic sensitivity or specificity.

Statistical analysis

Artifact maximal cord length and thickness was compared between image reconstructions using ANOVA and paired Student's t-tests and the relationship to BMI was tested using Pearson's correlation. The severity of artifacts was compared between image reconstructions by the Mann Whitney U test. Statistical significance was considered as $p < 0.05$ in a two-tailed distribution.

Results

Of the 246 thoracoabdominal rsDECT scans, 20 (8.1%) showed out-of-field body parts and comprised our study population. Out-of-field artifact was seen in all 20 patients at rsDECT. The mean age of these patients was 56 years (range, 28 to 72 years), and 14 were men and 6 women. The mean BMI of these 20 patients was 40.2 kg/m^2 (range, 26.9 to 61.7 kg/m^2).

The mean chord length of the artifact on axial images was 16.8 cm (range, 6.6 to 30.4 cm) and the mean z-axis length of the artifacts was 14.3 cm (range, 1.8 to 45 cm). The mean thickness of the out-of-field artifact was significantly thinner at iodine density images than at 65 keV images (0.68 ± 1.91 mm versus 8.31 ± 5.62 mm, respectively, p < 0.0001), or at other reconstructions (Table 1). Similarly, the mean severity of the out-of-field artifact was significantly less on iodine density images (0.25 ± 0.64) than on 65 keV (2.5 ± 0.8, p < 0.001) or other images (Table 1, Figs 2 and 3). In two of the 20 (10%) scans with out-of-field artifacts, the out-of-field artifacts obscured intraperitoneal anatomy. The thickness and chord length of the out-of-field artifact was significantly correlated for the 65 keV virtual monochromatic(r = 0.547, p<0.001), water density (r = 0.454, p<0.001) and iodine density images (r = 0.416, p<0.01). A larger BMI correlated with greater out-of-field artifact thickness (r = 0.712, p<0.001) (Figure 4). At virtual monochromatic images, the maximal thickness of the out-of-field artifact was smallest in the 40 keV images (mean, 4.25 mm), and greatest in 140 keV images (mean, 11.4 mm) (Table 1).

Discussion

We found out-of-field artifacts in 8% of our patients imaged with rsDECT scan. The majority of the patients with out-of-field artifacts had BMI > 30 kg/m^2, and all artifacts occurred in cases where body parts extended past the FOV, despite scanning with the maximum 50 cm FOV. We found that in all cases, the out-of-field artifacts were minimized at iodine density images compared to each of the other image reconstructions that we evaluated (virtual monochromatic 40, 65, and 140 keV, and water density images). The virtual monochromatic reconstruction with the least out-of-field artifact was the 40 keV setting.

Our findings contribute to the growing body of knowledge regarding the potential value of DECT to reduce artifacts that normally affect single energy CT scans. For example, a major benefit of DECT is to reduce metal artifact by use of virtual monochromatic high keV reconstructions (12, 13), or to emphasize iodine contrast signal at low keV reconstructions (14). Iodine density images have been shown to improve the detection of hypervascular liver lesions or hypovascular pancreatic lesions. Our findings build on this prior work by showing the benefit of iodine density images to minimize out-of-field artifact.

Physical limitations of radiological imaging of obese patients have become a common problem as the obesity epidemic continues to worsen in the United States and world (20–22). Several publications have advocated restricting DECT imaging to patients with low BMI or low girth (23–26). To our knowledge, ours is the first report that shows the potential benefit of rsDECT to image this problematic population of patients with large body habitus.

Many potential complications may occur in the outer-most portions of tissues in the obese patient, including abscesses of the breast, abdominal pannus, or lateral flank subcutaneous tissues, hernias, trauma, and catheter evaluation. Furthermore, CT frequently cannot image patients with limited mobility of their upper extremities optimally because their arms create out-of-field artifacts. In these populations, use of DECT with iodine density images may be helpful. It is important to note that the outer 2 cm annulus of a 50 cm circle comprises 15% of the total area of the circle. In other words, out-of-field artifact may obscure a substantial volume of the imaged field of view and interfere with clinical diagnoses.

The reason iodine density images improve out-of-field artifact at rsDECT is likely because artifacts of this type are inherent to the CT scanner design, and are largely unchanged between low and high kVp projections. This in turn causes them to appear in maximal severity in the water density image, as water also exhibits attenuation properties independent of X-ray energy within the diagnostic energy range (19). Correspondingly, they are largely absent in the iodine density image, as this image reconstruction shows projection data which exhibit a reduction in attenuation from low to high kVp. Our finding of lower artifact severity in the 40 keV compared to the 65 and 140 keV virtual monochromatic images is also explained because virtual monochromatic images are formed using the basis material decomposition of water and iodine (12, 27). The lower keV images are weighted more toward the iodine density map, while the higher keV images are weighted towards the water density map, hence the lower keV images thus show minimized out-of-field artifacts (personal communication with Saad Sirohey and Priti Madhav of GE Healthcare). This is contrary to DECT artifact reduction techniques for energy dependent artifacts such as metal and beam hardening. For these artifact types, the high keV virtual monochromatic images, which are weighted towards more penetrating high kVp projection data, show artifact suppression.

Our study has limitations. Firstly, our study is retrospective and from a single institution. Nevertheless, few other institutions utilize DECT imaging for large body habitus patients and so our findings add to the needed understanding of how DECT could potentially benefit medical diagnosis. We intend to further evaluate the underlying mechanisms for similar artifact reduction with DECT. Secondly, the small sample size only allowed us to make general observations and did not allow us to detail the value of iodine density images for the assessment of specific diseases. Nevertheless, each patient in our series served as their own control since several different DECT image reconstructions were compared. Larger sample sizes will allow further understanding of how out-of-field artifact reduction could benefit specific scenarios. Thirdly, we did not compare images from other types of dual energy CT scanners, such as the dual source, sandwich detector, twin-beam, or rotate-rotate platforms since these are not available at our institution. Further study will be needed on these other DECT implementations. Fourthly, the introduction of other artifacts, such as beam hardening (28), by iodine density images were not evaluated. Fifthly, since topogram images are not routinely saved in our CT scans, we did not assess the value of topograms for predicting the value of DECT reconstructions to improve out-of-field artifacts.

In conclusion, we found that the severity of out-of-field artifacts can be substantially reduced by the use of rsDECT iodine density images. Use of iodine density images may be of

particular value for obese or limb-paralyzed patients where regions of diagnostic interest are present at the edge of the scan FOV.
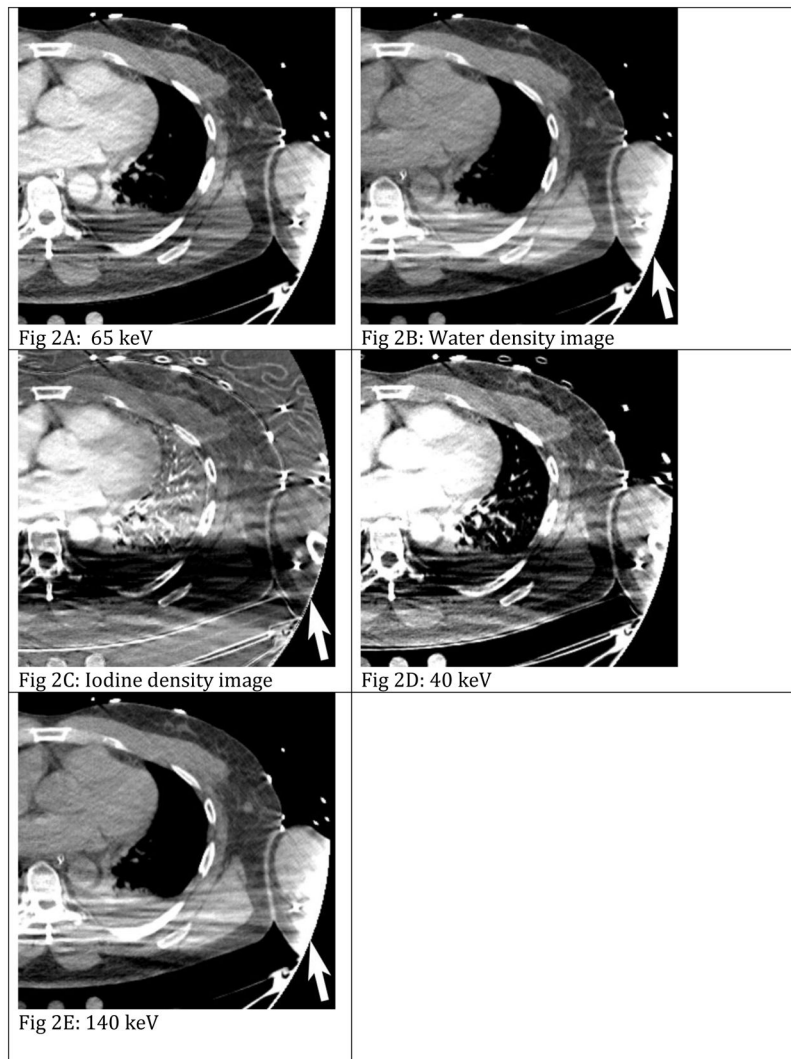
Acknowledgments

References

1. Bamberg F, Dierks A, Nikolaou K, Reiser MF, Becker CR, Johnson TR. Metal artifact reduction by dual energy computed tomography using monoenergetic extrapolation. Eur Radiol. 2011; 21:1424–1429. [PubMed: 21249370]

2. Kelly D, Hasegawa I, Borders R, Hatabu H, Boiselle P. High-resolution CT using MDCT: comparison of degree of motion artifact between volumetric and axial methods. Am J Roentgenol. 2004; 182:757–759. [PubMed: 14975982]

3. Brooks RA, Di Chiro G. Beam hardening in x-ray reconstructive tomography. Phys Med Biol. 1976; 21:390–398. published online EpubMay. [PubMed: 778862]

4. Barrett JF, Keat N. Artifacts in CT: recognition and avoidance. Radiographics. 2004; 24:1679–1691. published online EpubNov-Dec. DOI: 10.1148/rg.246045065 [PubMed: 15537976]

5. Ng M, Fleming T, Robinson M, Thomson B, Graetz N, Margono C, Mullany EC, Biryukov S, Abbafati C, Abera SF. Global, regional, and national prevalence of overweight and obesity in children and adults during 1980–2013: a systematic analysis for the Global Burden of Disease Study 2013. The Lancet. 2014; 384:766–781.

6. Ohnesorge B, Flohr T, Schwarz K, Heiken JP, Bae KT. Efficient correction for CT image artifacts caused by objects extending outside the scan field of view. Med Phys. 2000; 27:39–46. published online EpubJan. DOI: 10.1118/1.598855 [PubMed: 10659736]

7. Maltz, JS., Bose, S., Shukla, HP., Bani-Hashemi, AR. CT truncation artifact removal using water-equivalent thicknesses derived from truncated projection data. Conf. Proc. IEEE Eng. Med. Biol. Soc; 2007; 2007. p. 2907-2911.

8. Sourbelle K, Kachelriess M, Kalender WA. Reconstruction from truncated projections in CT using adaptive detruncation. Eur Radiol. 2005; 15:1008–1014. published online EpubMay. DOI: 10.1007/s00330-004-2621-9 [PubMed: 15702338]

9. Hsieh J, Chao E, Thibault J, Grekowicz B, Horst A, McOlash S, Myers TJ. A novel reconstruction algorithm to extend the CT scan field-of-view. Med Phys. 2004; 31:2385–2391. published online EpubSep. DOI: 10.1118/1.1776673 [PubMed: 15487717]

10. Marin D, Boll DT, Mileto A, Nelson RC. State of the art: dual-energy CT of the abdomen. Radiology. 2014; 271:327–342. published online EpubMay. DOI: 10.1148/radiol.14131480 [PubMed: 24761954]

11. Yu L, Leng S, McCollough CH. Dual-Energy CT–Based Monochromatic Imaging. Am J Roentgenol. 2012; 199:S9–S15. published online Epub2012/11/01. DOI: 10.2214/AJR.12.9121 [PubMed: 23097173]

12. Pessis E, Campagna R, Sverzut JM, Bach F, Rodallec M, Guerini H, Feydy A, Drapé JL. Virtual monochromatic spectral imaging with fast kilovoltage switching: Reduction of metal artifacts at CT. Radiographics. 2013; 33:573–583. [PubMed: 23479714]

13. Lee YH, Park KK, Song HT, Kim S, Suh JS. Metal artefact reduction in gemstone spectral imaging dual-energy CT with and without metal artefact reduction software. Eur Radiol. 2012; 22:1331–1340. [PubMed: 22307814]

14. Coursey CA, Nelson RC, Boll DT, Paulson EK, Ho LM, Neville AM, Marin D, Gupta RT, Schindera ST. Dual-energy multidetector CT: how does it work, what can it tell us, and when can we use it in abdominopelvic imaging? Radiographics. 2010; 30:1037–1055. published online EpubJul–Aug. DOI: 10.1148/rg.304095175 [PubMed: 20631367]

15. Ameli-Renani S, Rahman F, Nair A, Ramsay L, Bacon JL, Weller A, Sokhi HK, Devaraj A, Madden B, Vlahos I. Dual-energy CT for imaging of pulmonary hypertension: challenges and opportunities. Radiographics. 2014; 34:1769–1790. published online EpubNov–Dec. DOI: 10.1148/rg.347130085 [PubMed: 25384277]

16. Stiller W, Skornitzke S, Fritz F, Klauss M, Hansen J, Pahn G, Grenacher L, Kauczor HU. Correlation of quantitative dual-energy computed tomography iodine maps and abdominal computed tomography perfusion measurements: are single-acquisition dual-energy computed tomography iodine maps more than a reduced-dose surrogate of conventional computed tomography perfusion? Invest Radiol. 2015; 50:703–708. published online EpubOct. DOI: 10.1097/rli.0000000000000176 [PubMed: 26039774]

17. Silva AC, Morse BG, Hara AK, Paden RG, Hongo N, Pavlicek W. Dual-energy (spectral) CT: applications in abdominal imaging. Radiographics: a review publication of the Radiological Society of North America, Inc. 2011; 31:1031–1046. discussion 1047–1050. published online EpubJul–Aug. DOI: 10.1148/rg.314105159

18. Gupta S, Wagner-Bartak N, Jensen CT, Hui A, Wei W, Lertdilok P, Qayyum A, Tamm EP. Dual-energy CT of pancreatic adenocarcinoma: reproducibility of primary tumor measurements and assessment of tumor conspicuity and margin sharpness. Abdominal radiology (New York). 2016; Ahead of Print. published online EpubMar 8. doi: 10.1007/s00261-016-0689-8

19. Winklhofer S, Lambert JW, Wang ZJ, Sun Y, Gould RG, Zagoria RJ, Yeh BM. Reduction of peristalsis-related gastrointestinal streak artifacts with dual-energy CT: a patient and phantom study. Abdominal radiology (New York). 2016; Ahead of Print. published online EpubMar 17. doi: 10.1007/s00261-016-0702-2

20. Uppot RN, Sahani DV, Hahn PF, Kalra MK, Saini SS, Mueller PR. Effect of obesity on image quality: fifteen-year longitudinal study for evaluation of dictated radiology reports. Radiology. 2006; 240:435–439. published online EpubAug. DOI: 10.1148/radiol.2402051110 [PubMed: 16801372]

21. Reynolds A. Obesity and medical imaging challenges. Radiol Technol. 2011; 82:219–239. published online EpubJan-Feb. [PubMed: 21209424]

22. Carucci LR. Imaging obese patients: problems and solutions. Abdom Imaging. 2013; 38:630–646. published online EpubAug. DOI: 10.1007/s00261-012-9959-2 [PubMed: 23008055]

23. Karcaaltincaba M, Aktas A. Dual-energy CT revisited with multidetector CT: review of principles and clinical applications. Diagnostic and interventional radiology (Ankara, Turkey). 2011; 17:181–194. published online EpubSep. DOI: 10.4261/1305-3825.dir.3860-10.0

24. Guimaraes LS, Fletcher JG, Harmsen WS, Yu L, Siddiki H, Melton Z, Huprich JE, Hough D, Hartman R, McCollough CH. Appropriate patient selection at abdominal dual-energy CT using 80 kV: relationship between patient size, image noise, and image quality. Radiology. 2010; 257:732–742. published online EpubDec. DOI: 10.1148/radiol.10092016 [PubMed: 20959540]

25. De Cecco CN, Buffa V, Fedeli S, Luzietti M, Vallone A, Ruopoli R, Miele V, Rengo M, Paolantonio P, Maurizi Enrici M, Laghi A, David V. Dual energy CT (DECT) of the liver: conventional versus virtual unenhanced images. Eur Radiol. 2010; 20:2870–2875. published online EpubDec. DOI: 10.1007/s00330-010-1874-8 [PubMed: 20623126]

26. Yeh BM, Shepherd JA, Wang ZJ, Teh HS, Hartman R, Prevrhal S. Dual Energy and Low kVp CT in the Abdomen. AJR American journal of roentgenology. 2009; 193:47. [PubMed: 19542394]

27. Wu, X., Langan, DA., Xu, D., Benson, TM., Pack, JD., Schmitz, AM., Tkaczyk, EJ., Leverentz, J., Licato, P. Monochromatic CT image representation via fast switching dual kVp. Proc. SPIE 7258, Medical Imaging: Physics of Medical Imaging, 725845; March 13, 2009; 2009. p. 725845-725845-725849

28. Winklhofer S, Lambert JW, Wang ZJ, Sun Y, Gould RG, Zagoria RJ, Yeh BM. Reduction of peristalsis-related gastrointestinal streak artifacts with dual-energy CT: a patient and phantom study. Abdominal radiology. 2016; 41:1456–1465. published online EpubAug. DOI: 10.1007/s00261-016-0702-2 [PubMed: 26987848]
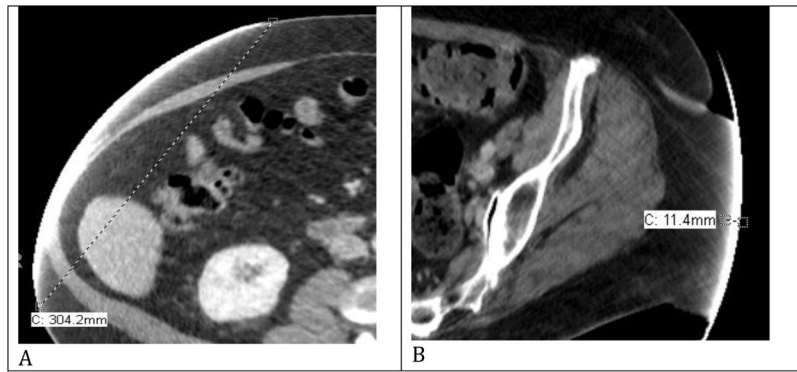
Figure 1.
Examples of measurements. A) Example measurement of maximal chord length of out-of-field artifact. The straight line distance of the out-of-field artifact was measured on the axial slice where the longest arc of artifact was seen. B) The thickness of bright out-of-field artifact was measured perpendicular to the circular curve of the field of view. Note: both images were cropped to better show the artifact measurements in these examples.

Fig 2A: 65 keV

Fig 2B: Water density image

Fig 2C: Iodine density image

Fig 2D: 40 keV

Fig 2E: 140 keV

Figure 2.
Arm out-of-field artifact.

A) 65 keV image shows out-of-field artifact on the left arm from tissue extending past the field of view. Artifact severity was recorded as 3 (obscures anatomy of subcutaneous fat and muscle, but not intraperitoneal or intrathoracic anatomy)

B) Water density image shows the worst artifact (arrow)

C) Iodine density image shows the least artifact, and best shows the bone, muscle, intravenous catheter, and arterial lumen of the left arm

D) 40 keV image shows less artifact than the E) 140 keV image (arrow)

Fig 3A: 65 keV

Fig 3B: Water density image

Fig 3C: Iodine density image

Fig 3D: 40 keV

Fig 3E: 140 keV
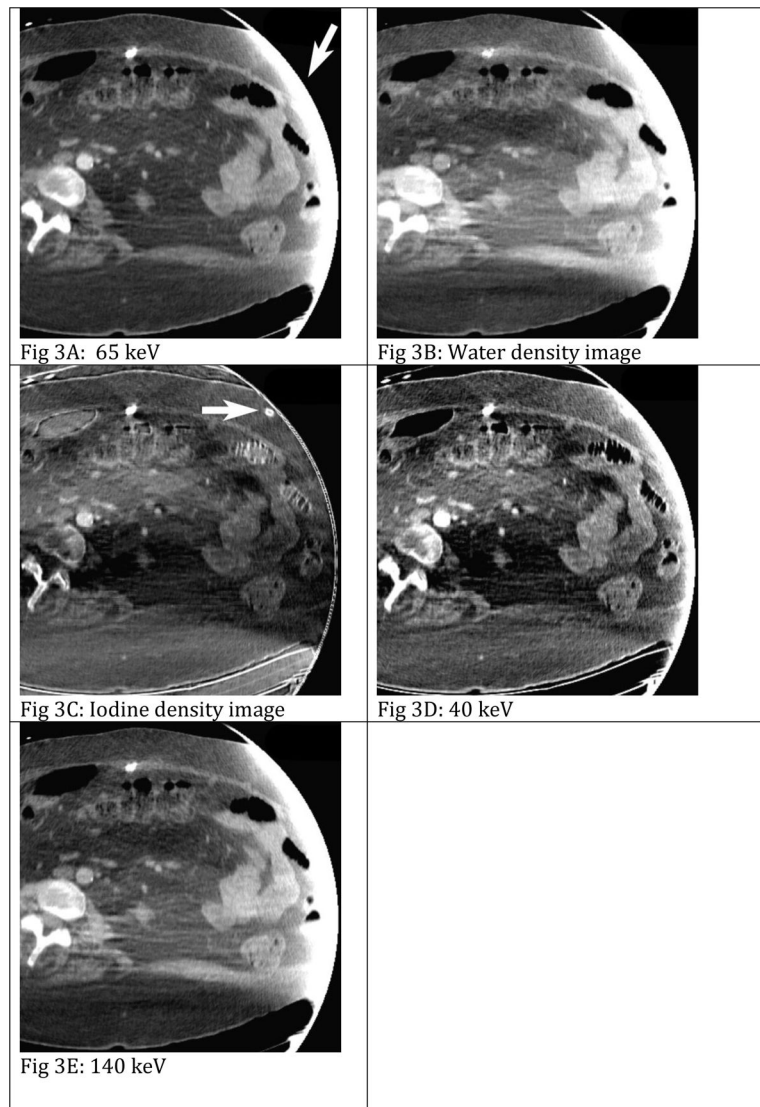
Figure 3.
Abdominal out-of-field artifact.

A) 65 keV image shows severe high signal artifact where the abdomen extends past the field of view (arrow). Some bowel and a portion of a drainage cathether are not seen. Severity score was 5.

B) Water density image shows severe artifact

C) Iodine density image shows absent out-of-field artifact and clearly shows drainage catheter (arrow) and surrounding tissue.

D) 40 keV image shows less out of field artifact than the E) 140 keV image.
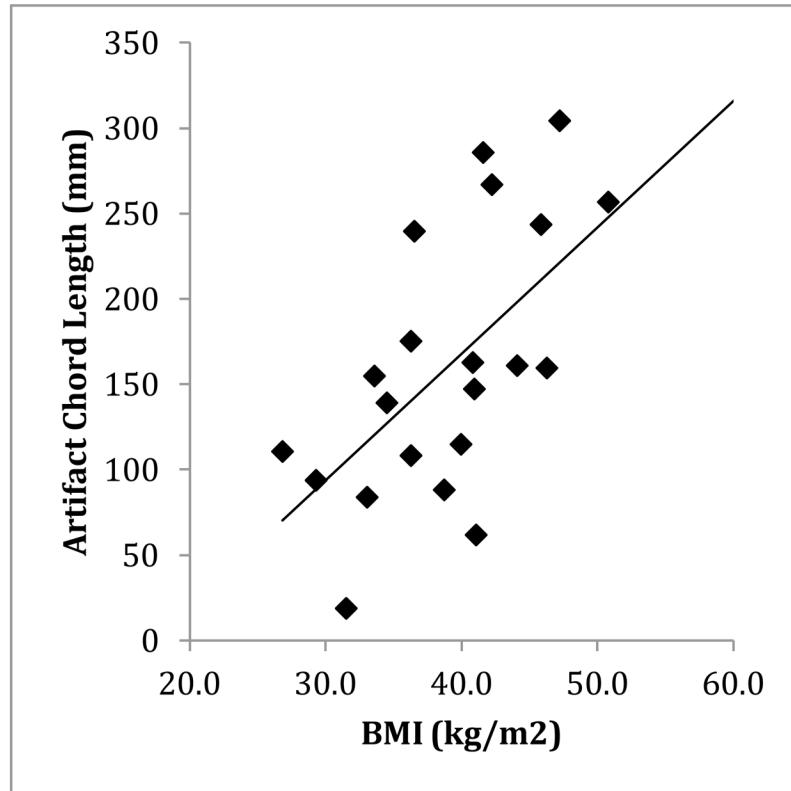
Figure 4.
Correlation between out-of-field artifact chord length and patient BMI. The correlation between out-of-field artifact chord length and patient BMI was r=0.712, p<0.001.
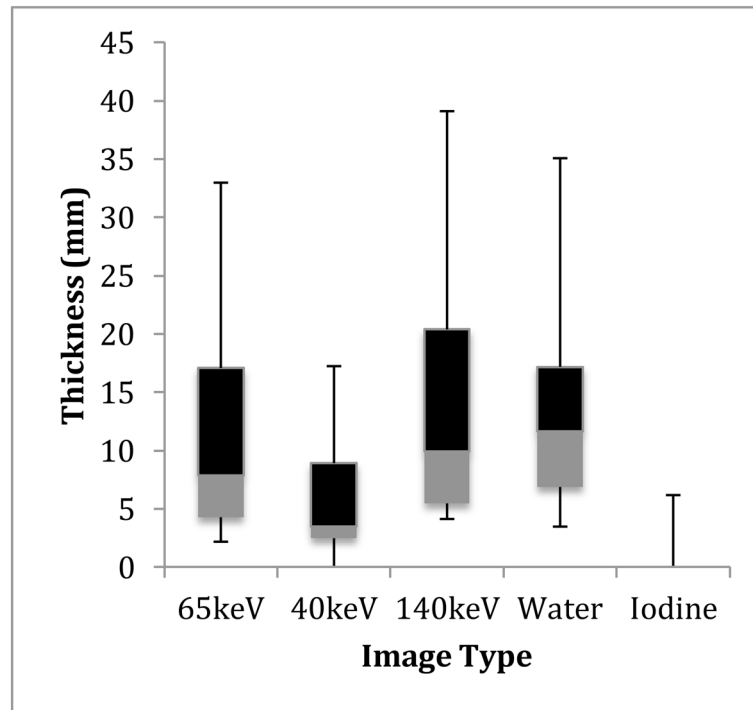
Figure 5.
Artifact thickness for 40, 65, and 140 keV virtual monochromatic images and water and iodine density images

Table 1

Thickness and severity of out-of-field artifact. Both the thickness and severity of out-of-field artifact were significantly worse for each image reconstruction (65, 40, and 140 keV virtual monochromatic images, and water density images) than for the iodine density images ($p < 0.001$ for each comparison)

	Thickness (mm)	Severity
65 keV	8.7 (3.5 to 27.3)	2.5 (2 to 3)
40 keV	4.7 (1.0 to 13.6)	2.3 (1 to 5)
140 keV	10.9 (3.0 to 31.0)	2.5 (2 to 5)
Water density image	13.4 (4.9 to 45.3)	2.7 (2 to 5)
Iodine density image	0.7 (0.0 to 6.2)	0.3 (0 to 2)